sulphonate groups, so that the closest oxygen to oxygen approach between groups is 3·06 Å. Similarly the O–S–O angles (mean 112° 45′) exceed the tetrahedral angle at the expense of the N–S–O angles (mean 105° 40′), so that the oxygen to oxygen separation within the sulphonate group is 2·40 Å, 0·1 Å less than the corresponding oxygen to nitrogen distance. The same effect was observed in the dinitrososulphite (O–S–O 115° 5′, O–S–N 104° 0′) and sulphamate (O–S–O 111° 30′, O–S–N 107° 30′) ions.

The interionic structure is illustrated in Fig. 8 which shows the projections down the principal crystallographic axes. The coordination of the ions is 12:6. An amine disulphonate ion II/V in Fig. 7(*a*), for example, is surrounded by twelve potassium ions: I, II, III, IV, V and VI in the same cell, II′, V′, VII and VIII in an adjacent cell, I and VI in the cell below. The closest interionic separations are the K · · · O values which range from 2·70 to 3·23 Å. The K · · · S distances are 3·50 Å and longer, and the K · · · N separations are somewhat greater (Table 3).

Table 3. *The shorter cation–anion interatomic distances*

(All values in Ångström units)

K · · · O_1	3·23(I)	2·74(II)	2·87(V)	
K · · · O_2	2·96(I′)	2·99(III)	3·07(VIII)	
K · · · O_3	2·71(I)	2·70(II)	2·84(VIII)	
K · · · S	3·51(I)	4·06(I′)	3·93(II)	3·84(II′)
	4·33(III)	4·04(V′)	3·49(VIII)	
K · · · N	3·82(I)	4·05(II)		

These distances refer to the cation K(I) and the roman numerals to those on the anions in Fig. 8 (a).

We are grateful to Prof. E. G. Cox for his interest and encouragement and to Dr D. W. J. Cruickshank and Dr P. J. Wheatley for the calculations with the Manchester electronic computer. We are indebted to the British Rayon Research Association for financial support to one of us (D. W. J.).

References

AHMED, F. R. & CRUICKSHANK, D. W. J. (1953). *Acta Cryst.* **6**, 765.

BERGLUND, E. (1876). *Bull. Soc. Chim.* (2), **25**, 452.

BROWN, C. J. & COX, E. G. (1940). *J. Chem. Soc.* p. 1.

COCHRAN, W. (1948). *J. Sci. Instrum.* **25**, 253.

COX, E. G., JEFFREY, G. A. & STADLER, H. P. (1949). *J. Chem. Soc.* p. 1783.

CRUICKSHANK, D. W. J. (1949). *Acta Cryst.* **2**, 65.

CRUICKSHANK, D. W. J. & ROBERTSON, A. P. (1953). *Acta Cryst.* **6**, 698.

CRUICKSHANK, D. W. J. & ROLLETT, J. S. (1953). *Acta Cryst.* **6**, 705.

JEFFREY, G. A. & STADLER, H. P. (1951). *J. Chem. Soc.* p. 1467.

JONES, D. W. (1955). *Acta Cryst.* **8**, 66.

MÜNZING, L. (1888). *Z. Kristallogr.* **14**, 62.

ROGERS, D. (1949). *Research, Lond.* **2**, 342.

SISLER, H. & AUDRIETH, L. F. (1938). *J. Amer. Chem. Soc.* **60**, 1947.

WAGNER, M. (1896). *Z. Phys. Chem.* **19**, 668.

WEISZ, O., COCHRAN, W. & COLE, W. F. (1947). *Acta Cryst.* **1**, 83.

WILSON, A. J. C. (1942). *Nature, Lond.* **150**, 152.

WILSON, A. J. C. (1949). *Research, Lond.* **2**, 246.

YOST, D. M. & RUSSELL, H. (1944). *Systematic Inorganic Chemistry of the Fifth- and Sixth-Group Non-Metallic Elements*, p. 98. New York: Prentice Hall.

ZIRNGIEBL, H. (1902). *Z. Kristallogr.* **36**, 117.

Acta Cryst. (1956). **9**, 289

Ordering of Atoms in the σ Phase*

BY J. S. KASPER AND R. M. WATERSTRAT

General Electric Research Laboratory, Schenectady, N.Y., U.S.A.

(*Received* 30 *September* 1955 *and in revised form* 31 *October* 1955)

A neutron diffraction study has been made of the ordering of component atoms in the following three σ phases: Ni–V, Fe–V, Mn–Cr. Definite evidence for ordering is found in all three systems, with different degrees of precision for the three systems. These results, with some X-ray investigations, enable a generalization to be made regarding the scheme of the ordering for binary σ phases of the first row transition elements (also those containing molybdenum).

Introduction

In recent years there have been detailed X-ray diffraction investigations of the structure of the σ phase in which the locations of the atoms in the unit cell have been made with considerable precision (Bergman & Shoemaker, 1954; Dickins, Douglas & Taylor, 1956; Kasper & Decker, 1955). It has not been possible in these studies, however, to decide whether there is a definite ordering of the respective atoms among the different sites in the unit cell

* The neutron diffraction data were obtained at the Brookhaven National Laboratory Reactor, Upton, L. I., N.Y., U.S.A.

because of the extreme closeness of the X-ray scattering factors concerned (those for Fe and Cr or for Co and Cr). Only powder methods could be used for the more favorable cases such as Mn–Mo (Decker, Waterstrat & Kasper, 1954) and Fe–Mo (Bergman & Shoemaker, 1954), with the result that the characterization of the ordering could not be made completely. On the other hand the weak extra reflections for Ni–V, which were interpreted as indicating an ordering, have been shown to arise from the 'double reflection' effect (Bland, 1954).

A consideration of neutron scattering factors immediately suggests the advantages of neutron diffraction for elucidating the question of ordering. The system Ni–V is especially favorable, since in this instance there is the simultaneous occurrence of the largest scatterer for neutrons (Ni) and the lowest (V), the latter essentially negligible for coherent scattering. The Fe–V and Mn–Cr systems appear attractive also, as indicated by the following scattering factors:

$$b_{Ni} = 1{\cdot}03,\ b_{Fe} = 0{\cdot}96,\ b_{V} = -0{\cdot}048,\ b_{Mn} = -0{\cdot}37,\ b_{Cr} = 0{\cdot}352 \text{ cm}.$$

Consequently we have made a neutron diffraction examination of each of the three binary systems mentioned above. In each of them we find clear-cut evidence for ordering and are able to deduce its nature quite exactly, despite the fact that only powdered specimens were used and notwithstanding the complexity of the structure.

We have assumed that the atomic parameters in all cases were the same as those found in the single-crystal studies that have been made most carefully, where there is very good agreement among the independent investigators. In further support of this procedure is the fact that among the binary σ phases of first-row transition elements there is remarkable agreement of corresponding intensities in the X-ray diffraction patterns. Also, parameter variations have only a very minor effect on the neutron intensities relative to the effects of ordering. The exact parameters used were those found in this laboratory for Co–Cr σ, which were for space group D_{4h}^{14}–$P4/mnm$, with 5 crystallographically different kinds of atoms, as follows:

I	2(*b*);	
II	4(*f*),	$x = 0{\cdot}103$;
III	8(*i*),	$x = 0{\cdot}371,\ y = 0{\cdot}037$;
IV	8(*i*),	$x = 0{\cdot}566,\ y = 0{\cdot}240$;
V	8(*j*),	$x = 0{\cdot}316,\ z = 0{\cdot}250$.

Neutron diffraction measurements

The neutron diffraction patterns were obtained in a uniform manner for all specimens. Fine powdered material (ground to 200 mesh size) was contained in flat cells with glass windows of cross-section $2\frac{3}{4}$ in. × $4\frac{1}{2}$ in. The thickness of the cell was either $\frac{1}{2}$ in. or $\frac{3}{8}$ in. The neutron beam, 2 in. × 2 in. in cross-section, was monochromatized by reflection from a single crystal of lead and collimated by Soller slits. Its wave-length was 1·023 Å. except for one experiment ($Ni_{13}V_{17}$) where it was 1·054 Å. The incident beam was monitored so that for each angular setting of the BF_3 detector the recorded diffracted intensity was for a constant number of incident neutrons. Integrated intensities were obtained by measuring the areas under peaks with a planimeter.

The calculations of integrated intensity P_{hkl} were made from the expression appropriate for a flat powder specimen,

$$P_{hkl} = K \frac{t\varrho'}{\varrho} \frac{e^{-\mu t \sec\theta}}{\sin^2 2\theta} j_{hkl} N_c^2 F_{hkl}^2 ,$$

where θ is the Bragg angle, j_{hkl} the multiplicity, F_{hkl} the crystal structure factor, t the thickness of the specimen, and μ its absorption coefficient, ϱ' the measured density of the specimen, ϱ the theoretical density and N_c the number of unit cells per cubic centimetre. Instrumental constants are included in K, which was evaluated by measuring the diffraction pattern of a nickel standard. Consequently, the integrated intensities were on an absolute basis, except where noted.

Ni–V

Three different compositions within the σ homogeneity range were studied. They shall be designated by the formulas Ni_9V_{21}, $Ni_{11}V_{19}$, $Ni_{13}V_{17}$. The exact compositions, cell constants and densities are given in Table 1.

Table 1. Ni–V σ *phase*

	A		*B*		*C*	
Specimen	Ni	V	Ni	V	Ni	V
Nominal weight %	33	67	38	62	46	54
Chemical analysis weight %	33·1	66·8	38·3	61·7	46·7	53·2
Atomic %	30·1	69·9	35·0	65·0	43·2	56·8
*Z**	9·0	21·0	10·5	19·5	13·0	17·0
a_0 (Å)	9·04		8·98		8·95	
c_0 (Å)	4·67		4·64		4·63	
c/a	0·517		0·517		0·517	
ϱ_c (g.cm.$^{-3}$)	7·011		7·198		7·338	

* Number of atoms in unit cell.

The alloys were prepared from carbonyl nickel (99·9%) and pure ductile vanadium (99·8%) by arc melting twice in an argon atmosphere. The specimens were then crushed in a rod mill to 200 mesh size and annealed at 500° C. for 120 hr. X-ray diffraction photographs showed the σ pattern with no positive indication of free nickel or vanadium.

Analysis of neutron diffraction pattern

The neutron diffraction patterns of the three specimens at 25° C. are shown in Fig. 1. For comparison purposes, an X-ray diffraction trace of a typical

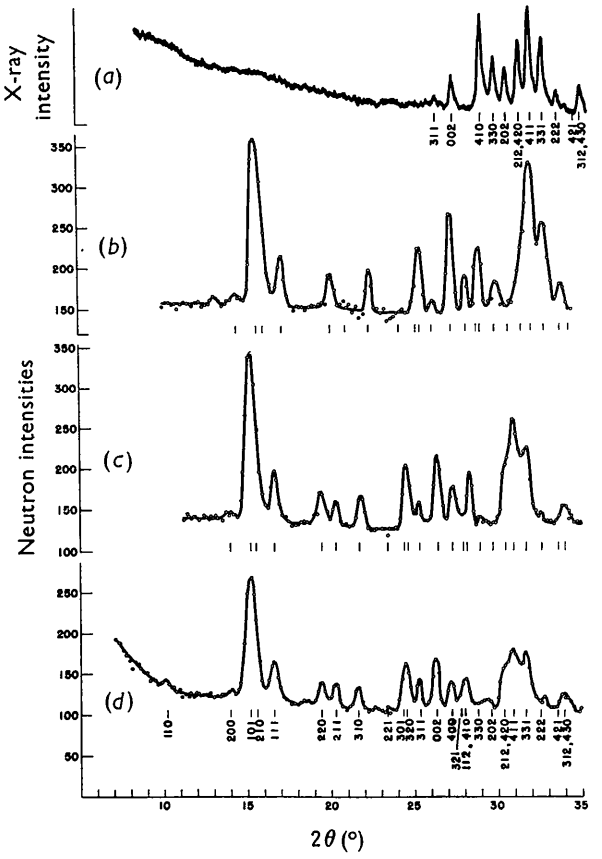

Fig. 1. Comparison of neutron diffraction patterns of Ni–V σ phases with an X-ray trace of Mn–Cr σ phase.
(*a*) Typical σ-phase X-ray trace (Mn–Cr). (*b*)–(*d*) Neutron diffraction patterns of Ni–V σ phase: (*b*) $Ni_{13}V_{17}$, (*c*) $Ni_{11}V_{19}$, (*d*) Ni_9V_{21}.

σ-phase pattern* is also included in Fig. 1. Since in the X-ray case the scattering factors are essentially equal, this same pattern would be expected for neutron diffraction, *if the respective atoms were distributed randomly among the crystallographic sites*. Fig. 1 demonstrates very effectively that the distribution of the two kinds of atoms is not random.

Since the vanadium scattering factor is practically negligible compared to that of nickel, the neutron intensities are determined essentially by the distribution of the nickel atoms. Elementary considerations of the contributions to the structure factor associated with each of the five positions in the σ-phase unit cell lead to a definite conclusion that positions I and IV must be almost exclusively occupied by nickel atoms. For instance, this is required in order to achieve the high intensity observed for the (101)+(210) combined peak, which would be hardly observable for a random distribution of atoms.

A more objective procedure was also followed. From the absolute intensity of (002) it is possible to decide directly the number of Ni atoms in position V. The (002) reflection is independent of the structural parameters, and its structure factor is given simply by the number of atoms in positions other than V minus the number of atoms in V. Then, there are the reflections of the type *h*, *k*, *l* all odd which involve only positions II, III, IV. A simultaneous-equations solution could be made on these for the effective scattering factor for each position. A reasonably consistent set of numbers could be arrived at, in this manner, and these gave good but not excellent intensity correlation. These values served, finally, to allow a least-squares treatment of the observed intensities for the best values of the effective scattering factors for each of the five positions in the unit cell. The number of nickel and vanadium atoms associated with each position follows directly from the effective scattering factors for the positions and the known scattering factors for the elements. The results of this procedure are given in Table 2. There is some question regarding the applicability of the least-squares method for the specimen $Ni_{13}V_{17}$. This specimen was investigated at a different time from the other two, and for it there is uncertainty regarding the instrumental factors which are required to place the intensities on an absolute basis. None the less, the method was applied here with the best evaluation of the intensity scale factor possible, since it was believed that the preference of nickel for the different sites would still be indicated, although the

* The Mn–Cr σ pattern was selected merely because of its better quality. The Ni–V pattern is not significantly different as to distribution of intensity, but it is not as well suited for illustrative purposes.

Table 2. *Distribution of atoms in* Ni–V σ *phases from least-squares fitting of neutron intensities*

Atom type	Number in unit cell	Ni_9V_{21}		$Ni_{11}V_{19}$		$Ni_{13}V_{17}$	
		Effective *b*	No. of Ni	Effective *b*	No. of Ni	Effective *b*	No. of Ni
I	2	0·850	1·7	0·900	1·8	0·837	1·7
II	4	−0·030	0·1	−0·110	0·0	−0·078	0·0
III	8	0·024	0·5	0·150	1·5	0·270	2·4
IV	8	0·883	6·9	0·929	7·3	0·901	7·0
V	8	−0·033	0·1	−0·033	0·1	0·023	0·5
	Total No. of Ni		9·3		10·7		11·6
	No. of Ni from analysis		9·0		10·5		13·0

$b_{Ni} = 1{\cdot}03$, $b_V = -0{\cdot}048$.

actual number of nickel atoms deduced might be in error. Actually, a very good intensity correlation is obtained for $Ni_{13}V_{17}$ on a relative basis if the 13 nickel atoms are distributed as follows: 2 in I, 8 in IV, and 3 in III. Since the analysis calls for 13 nickel atoms, we have used the latter distribution for the comparison of intensities in Table 3.

For the specimens Ni_9V_{21} and $Ni_{11}V_{19}$, where there is no reason to question the absolute scale determination, there is good agreement for the total numbers of nickel atoms with the known composition as well as a consistency in the results. Thus, there is clearly the strong, but not complete, preference of nickel for positions I and IV, with position III as the next position of preference and the absence of nickel in position II. It is to be noted that for position II the effective b calculated for $Ni_{11}V_{19}$ (and for $Ni_{13}V_{17}$) is lower significantly than the limiting value of $-0{\cdot}048$ for vanadium. While this strongly suggests that no nickel is in II, it also indicates that the number of atoms deduced is uncertain to about 0·2. It does appear real, however, that positions I and IV are not exclusively filled by nickel. For this possibility the calculated intensities are significantly poorer than with the distribution given in Table 2.

With regard to the slight deviation from complete occupation of I and IV by nickel, it is not possible to say whether this is an equilibrium situation. The specimens were not given very long annealing times and it may be that complete ordering has not been attained. It is contemplated to check this possibility with specimens which have been more extensively annealed.

Table 3. *Comparison of observed and calculated neutron intensities for* Ni–V σ *phases*

	Ni_9V_{21}		$Ni_{11}V_{19}$		$Ni_{13}V_{17}$	
hkl	I_o	I_c	I_o	I_c	I_o	I_c
110	8	9	0	2	0	2
200	7	4	7	8	18	19
101, 210	201	231	266	278	258	259
111	53	53	54	60	51	48
220	26	24	38	30	30	29
211	20	20	20	16	0	6
310	21	23	28	30	30	34
221	0	1	0	0	0	1
301, 320	55	63	64	67	65	56
311	23	22	19	20	15	11
002	50	53	77	80	90	100
400, 321	31	33	36	37	33	30
112, 410	39	31	45	44	61	54
330, 202	0	4	7	11	35	19
212, 420	44	51	59	58	46	40
411	73	87	120	141	184	187
331, 222	93	88	105	122	122	118
421	0	1	0	2	6	7
312, 430, 510	21	25	—	—	33	39

The agreement between observed and calculated intensities is given in Table 3. For the reasons discussed above, in the case of $Ni_{13}V_{17}$ the intensities are on a relative basis, but the comparison is made on an absolute basis for the other two specimens. In view of the complexity of the structure the intensity agreement appears quite satisfactory. There remains to be considered the effect of a change in the atomic parameters from those used. It is, of course, not possible from these data to ascertain exact parameters. The effect of parameter changes was investigated, however, and it was established that quite large changes (of the order of 0·01) would not materially affect the distribution of atoms deduced here.

Considering all three specimens it is possible to describe the scheme of ordering as follows:

Atom type

I	Essentially all nickel.
II	All vanadium.
III	Contains essentially all nickel above that required to fill I and IV.
IV	Essentially all nickel.
V	Essentially all vanadium.

Fe–V

The iron-vanadium σ phase also is very favorable for a determination by neutron diffraction of the distribution of the component atoms among the sites in the unit cell. Accordingly, upon finding the definite ordering in nickel–vanadium σ's, we have made preliminary investigations in the iron–vanadium system. The source material was ferrovanadium with an analysis corresponding very closely to the composition $Fe_{12}V_{18}$ with about 1·5% silicon impurity. This material was homogenized for 100 hr. at 1000° C., then crushed, and the powder was annealed at 700° C. for 70 hr. The X-ray diffraction photographs showed the σ pattern with no evidence for appreciable amounts of impurity. There appear in the neutron diffraction pattern, however, at least two small peaks that do not index for the σ structure. Since the specimen is somewhat impure, the data may not be sufficiently reliable to warrant a least-squares analysis for the atomic ordering. None the less, there is clear-cut evidence for an ordering of atoms, and the main features of the scheme of ordering can be definitely deduced.

The neutron diffraction experiments were performed in the manner described for nickel–vanadium and the methods of treating the information were also similar. The intensities reported for iron–vanadium are on an absolute basis.

The neutron diffraction pattern of the iron–vanadium σ at 25° C., shown in Fig. 2, bears a strong resemblance to those of the nickel–vanadium alloys, and this suggests a similarity in the arrangement of iron

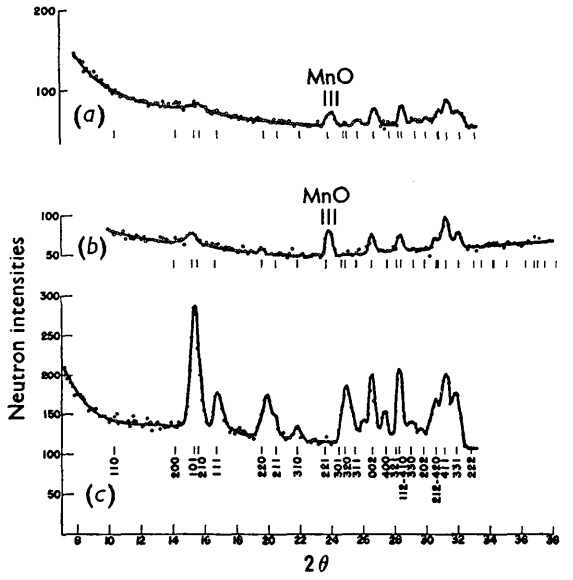

Fig. 2. Neutron diffraction patterns of Mn–Cr and Fe–V σ phases.
(a) Mn–Cr σ phase (75% Mn, 25% Cr) quenched from 1100° C.
(b) Mn–Cr σ phase (75% Mn, 25% Cr) annealed at 850° C.
(c) Fe–V σ phase ($Fe_{12}V_{18}$).

atoms versus nickel atoms in the two cases. A random arrangement is, of course, clearly ruled out. As with nickel–vanadium, it can be readily ascertained that the pattern calls for a high concentration of the strong scatterer (iron) in positions I and IV. There appears to be no iron in position II and a small amount in position III. Again, there is a similarity here to the distribution of nickel in NiV. A more detailed consideration of the intensities indicates, however, that, unlike nickel in NiV, there is presence of iron in position V.

By trial and error it was found that the distribution of atoms given in Table 4 gave a satisfactory agreement of observed and calculated intensities (Table 5), which we could not improve upon. While we believe this distribution to be essentially correct, it is planned to obtain further information from samples of iron–vanadium σ which are made more carefully.

Because of the reported magnetism (Nevitt & Beck, 1955) at low temperatures, and since FeV has the highest Curie point (203° K.) of the σ phases investigated, we have obtained neutron diffraction patterns also at 77° K. and 47° K. There appears to be no difference in the patterns at the three temperatures. The sample investigated by Nevitt & Beck was

Table 4. *Distribution of iron atoms in* Fe–V σ *phase*

1·7 Fe in I,	b_I	= 0·86 cm.
0 Fe in II,	b_{II}	= −0·048
1·5 Fe in III,	b_{III}	= 0·142
6·8 Fe in IV,	b_{IV}	= 0·816
2 Fe in V,	b_V	= 0·204

Table 5. *Comparison of observed and calculated neutron intensities for* Fe–V σ *phase at* 25° C.

	I_o	I_c
110	0	4
200	0	0·03
110, 210	173	203
111	55	51
220	25	13
211	25	12
310	18	14
221	0	0·1
301, 320, 311	96*	65
002	55	45
400	30	27
321, 112, 410	90	83
330	33	27
202	24	12
212, 420	93	96
411	109	125
331	90	91
222	13	27
421	0	0·3

* This abnormal value was observed only at room-temperature. At 77° K. the intensity observed was ~ 70.

of the composition $Fe_{15·7}V_{14·3}$. We have subsequently verified that there is appreciable magnetism for this composition, but none detectable even at 4·2° K. for compositions as low in iron content as the one studied here.

Mn–Cr

A specimen of composition corresponding to Mn_3Cr (75·4 atomic% Mn, 24·6% Cr by analysis) was prepared by melting in a resistance furnace under 1 atmosphere of argon from electrolytic manganese and electrolytic chromium. It was homogenized for 3 hr. at 1100° C. in dry hydrogen and then quenched in cold water. After the neutron diffraction pattern was obtained this specimen was then annealed for 24 hr. at 850° C. and again examined by neutron diffraction. It was hoped to ascertain thereby whether an atomic redistribution was responsible for the transition at 998° C. reported by Pearson & Hume-Rothery (1953). They report a heat of transformation but no detectable difference in the X-ray patterns below and above this temperature.

The neutron diffraction pattern for a completely random distribution of the respective atoms of this σ would consist of only weak peaks because of the cancelling effect of the scattering factors (b_{Mn} = −0·37, b_{Cr} = +0·352). Also, for many non-random distributions of atoms only weak peaks would occur, although these patterns in general would differ recognizably from that for the random situation. It turns out that for the Mn–Cr σ the patterns (Fig. 2) are weak and consequently the distribution of atoms cannot be specified as precisely as in the Ni–V and

Fe–V σ's. Furthermore, there is some contamination by MnO, as indicated in the patterns of Fig. 2. None the less, there appears to be a difference in the quenched and annealed states, and the distribution in the latter can be deduced with some definiteness.

Table 6. *Comparison of observed and calculated neutron intensities for* Mn–Cr σ *phase*

	Quenched	Annealed	Disordered	Ordered
hkl	I_o	I_o*	I_c	I_c
110	0	0	< 0·1	3
200	0	0	< 0·1	1
101, 210	5	21	0·4	23
111	0	0	0·1	4
220	0	0	0·1	2
211	0	0	0·1	3
310	0	0	0·1	2
221	—†	—†	0·1	1
301	0	0	0	4
320	0	0	0	1
311	5	0	2	0·2
002	17	15	7	15
400	0	0	0	2
321, 112, 410	17	15	26	15
330	6	0	11	4
202	8	0	11	3
212, 420	18	17	22	15
411	30	37	34	36
331	15	23	17	25
222	0	0	0·1	3

* A zero value here represents an intensity < 5.
† Covered by MnO peak.

In Table 6 are given the observed intensities and also those calculated for a disordered arrangement and for the arrangement giving best agreement with the observed values for the annealed specimen. The intensities of the quenched specimen do not differ greatly from those for the disordered situation, although there is not complete agreement. It does not seem profitable to attempt an exact analysis of the deviation from random distribution for this case. It is seen, however, that this deviation is more marked for the annealed specimen, especially in the growth of the (101)+(210) intensity and the decrease of (330) and (202) peaks. The trial of models is facilitated by the use of (002) to give directly the distribution in positions V. Thus, for the annealed specimen the absolute intensity of (002) calls for 3–3·5 chromium atoms in positions V. By trial it is ascertained that discrepancies in intensities occur if any appreciable amount of chromium (> 0·5 atom) is associated with positions I and IV. The best fit found, with the intensities in Table 6, is for the following model:

Position	No. of Cr	No. of Mn
I	0	2
II	1	3
III	3	5
IV	0	8
V	3·5	4·5

From the sensitivity of intensity to distribution, it would seem that the numbers above are correct to 0·5. While there is no one position exclusively occupied by chromium atoms, there is definite preference by them for positions III and V, with essentially no occupancy of positions I and IV.

It is interesting to compare this system to the Mn–Mo σ (Decker *et al.*, 1954), where there is the substitution of the minor constituent (Cr) by an element in the same column of the periodic table (Mo). Here the molybdenum atoms fill position II essentially completely, and with the remainder distributed among positions III and V. There is the similarity of the two systems, however, in that no molybdenum atoms are found in positions I and IV.

Conclusion

In each of the σ phases that we have studied, there is indicated to be an 'ordering' of atoms in the sense that there are preferences of a given kind of atom for certain of the crystallographic sites in the unit cell. The results of this investigation combined with those of the X-ray studies on Mn–Mo (Decker *et al.*, 1954), Co–Cr (Dickens *et al.*, 1956; Kasper & Decker, 1955) and Fe–Cr (Bergman & Shoemaker, 1954) σ's, allow a generalization to be made regarding the nature of this ordering for binary σ phases containing first long-row elements and also molybdenum. For this generalization, we may consider the elements as divided into two groups according to their occurrence in the periodic table relative to manganese. Thus, those to the left of manganese (V, Cr, Mo) we shall designate as *A* and those to the right (Fe, Co, Ni) as *B* elements. Manganese appears anomalous in needing to be considered in both groups, even in the same σ. The generalization, then, in terms of the crystallographic positions of the unit cell, as designated throughout this paper, is:

Position	Coordination number	Occupancy
I	12	*B*
II	15	*A*
III	14	Mixed
IV	12	*B*
V	14	Mixed

For a given σ phase there does not appear to be the complete correspondence of a position with the kind of atom for all positions. On the other hand, there is that correspondence generally for positions I, II and IV. The extensiveness of the homogeneity range is then related to the accommodation of varying proportions of the component atoms in positions III and V.

It is interesting that there is a correlation of the scheme of ordering with coordination number. Thus, the positions occupied by *B* atoms (I and IV) are those of lowest coordination, namely 12, corresponding to slightly distorted regular icosahedra; the position (II) of highest coordination (15) is occupied by *A* atoms;

and the mixed occupancy occurs in the two positions of intermediate coordination number (14).

We gratefully acknowledge helpful discussions and suggestions by Mrs B. F. Decker.

References

BERGMAN, G. & SHOEMAKER, D. P. (1954). *Acta Cryst.* **7**, 857.

BLAND, J. A. (1954). *Acta Cryst.* **7**, 477.

DECKER, B. F., WATERSTRAT, R. M. & KASPER, J. S. (1954). *J. Metals, N.Y.* **6**, 1406.

DICKINS, G. J., DOUGLAS, A. M. B. & TAYLOR, W. H. (1956). *Acta cryst.* **9**, 297.

KASPER, J. S. & DECKER, B. F. (1955). Unpublished results.

NEVITT, M. V. & BECK, P. A. (1955). *J. Metals, N.Y.* **7**, 669.

PEARSON, W. B. & HUME-ROTHERY, W. (1953). *J. Inst. Met.* **81**, 311.

Acta Cryst. (1956). **9**, 295

A Crystallographic Study of the Tellurium–Iodine System*

BY W. R. BLACKMORE†, S. C. ABRAHAMS‡ AND J. KALNAJS

Laboratory for Insulation Research, Massachusetts Institute of Technology, Cambridge, Massachusetts, U.S.A. and Chemistry Department, The University, Glasgow W. 2, Scotland

(*Received* 12 *December* 1955)

Crystallographic data are given for the two stoichiometric compounds formed within the tellurium–iodine system. Tellurium tetraiodide crystallizes in the orthorhombic system with $a = 13{\cdot}54 \pm 0{\cdot}02$, $b = 16{\cdot}73 \pm 0{\cdot}02$ and $c = 14{\cdot}48 \pm 0{\cdot}02$ Å, space group *Pnma* or $Pn2_1a$. The other composition corresponds to Te_nI_n, and also crystallizes in the orthorhombic system, with $a = 8{\cdot}23 \pm 0{\cdot}03$, $b = 30{\cdot}00 \pm 0{\cdot}05$ and $c = 9{\cdot}97 \pm 0{\cdot}03$ Å, space group *Cmma* or *Cm2a*. The structure of a tetragonal crystal which may have been tellurium tetraiodide is described.

Introduction

The lattice constants of the terminal members of the tellurium–iodine system are well known. Tellurium is hexagonal with

$$a = 4{\cdot}45564 \pm 0{\cdot}00012,$$
$$c = 5{\cdot}92685 \pm 0{\cdot}00002 \text{ Å at } 18° \text{ C}.$$

(Straumanis, 1940) and iodine is orthorhombic with

$$a = 4{\cdot}784 \pm 0{\cdot}001,\ b = 7{\cdot}265 \pm 0{\cdot}001 \text{ and}$$
$$c = 9{\cdot}792 \pm 0{\cdot}002 \text{ Å}$$

(Heavens & Cheesman, 1950). Within this system, until the present investigation, the only well established stoichiometric compound had been tellurium tetraiodide. The structure of tellurium tetraiodide is of interest in a current study of 2-, 3- and 4-bonded compounds of the subgroup VI*b* elements. It was also thought desirable to re-examine the tellurium–iodine system by X-ray methods, even although the phase diagram had previously been investigated by thermal analysis (Jaeger & Menke, 1912; Damiens, 1923).

* Sponsored in part by the Office of Naval Research, the Army Signal Corps and the Air Force under ONR Contract N5ori-07801.

† Present address: Central Research Laboratory, Canadian Industries (1954) Limited, McMasterville, Quebec, Canada.

‡ Present address: Chemistry Department, The University, Glasgow W. 2, Scotland.

Experimental

Crystalline tellurium tetraiodide was prepared either by heating tellurium tetrabromide with ethyl iodide (Montignie, 1947) or by reacting the elements in a modification of Damiens' (1923) method. In this modification, the elements are mixed in the requisite proportions, and sealed off in a small-volume Pyrex tube in an atmosphere of nitrogen. Since tellurium melts at 452° C., the tube is heated to about 500° C. for 2–3 hr., to ensure completion of the reaction. The resulting black crystals of tellurium tetraiodide take the form of plates and bipyramids.

Intermediate compositions were prepared in the same manner, from the melt. The preparation corresponding to Te_nI_n was further annealed for 15 hr. at about 120° C. and cooled slowly to promote crystal growth.

The single-crystal X-ray diffraction measurements were recorded using Weissenberg and precession cameras with Mo $K\alpha$ ($\lambda = 0{\cdot}7107$ Å) radiation. With microcrystalline samples, the Norelco wide-range diffractometer and also the 114·59 mm. diameter powder camera were used with Cu $K\alpha$ ($\lambda = 1{\cdot}5418$ Å) radiation.

Crystal data for orthorhombic tellurium tetraiodide

All preparations except that referred to in the foot-